OLD DOMINION UNIVERSITY RESEARCH FOUNDATION

SCHOOL OF ENGINEERING
OLD DOMINION UNIVERSITY
NORFOLK, VIRGINIA

(NASA-CR-154648) INVESTIGATION OF AN INCOMPRESSIBLE FLOW ALONG A CORNER BY AN ALTERNATING DIRECTION IMPLICIT METHOD Final Report (Old Dominion Univ. Research Foundation) 52 p HC A04/MF A01 CSCL 20D G3/34

N77-30409

Unclas
42070

INVESTIGATION OF AN INCOMPRESSIBLE FLOW ALONG A CORNER BY AN ALTERNATING DIRECTION IMPLICIT METHOD

By

Dashrath K. Patel

G.L. Goglia, Principal Investigator

Final Report

Prepared for the
National Aeronautics and Space Administration
Langley Research Center
Hampton, Virginia

Under
Research Grant NSG 1311
Percy J. Bobbitt, Technical Monitor
Theoretical Aerodynamics Branch
Subsonic-Transonic Aerodynamics Division

SEP 1977
RECEIVED
NASA STI FACILITY
INPUT BRANCH

August 1977

Old Dominion University Research Foundation
Norfolk, Virginia 23508
Phone 804/489-6624

September 8, 1977

Mr. Percy J. Bobbitt
National Aeronautics and Space Administration
Langley Research Center - Mail Code 360
Hampton, VA 23665

Dear Mr. Bobbitt:

Reference research grant NSG 1311, G.L. Goglia principal investigator.

Enclosed is the final technical report on work performed under the referenced grant.

If there are any questions on the report, please contact this office.

Sincerely,

Maxine Lippman
Publications Coordinator

Encl: Fin Rpt, 3 cys

cc: NASA Sci & Tech Info Fac, 2 cys
Dr. Patel, 10 cys
Dr. Goglia, 3 cys
ODU Library, 1 cy
Mr. Kawalkiewicz, ltr only

/mal

SCHOOL OF ENGINEERING
OLD DOMINION UNIVERSITY
NORFOLK, VIRGINIA

INVESTIGATION OF AN INCOMPRESSIBLE FLOW ALONG A CORNER BY AN ALTERNATING DIRECTION IMPLICIT METHOD

By

Dashrath K. Patel

G.L. Goglia, Principal Investigator

Final Report

Prepared for the
National Aeronautics and Space Administration
Langley Research Center
Hampton, Virginia 23665

Under
Research Grant NSG 1311
Percy J. Bobbitt, Technical Monitor
Theoretical Aerodynamics Branch
Subsonic-Transonic Aerodynamics Division

Submitted by the
Old Dominion University Research Foundation
Norfolk, Virginia 23508

August 1977

ABSTRACT

The axial corner flow is analyzed for the imcompressible laminar boundary layer flow. The governing equations are derived from the Navier-Stokes equations by neglecting second derivative terms of the axial direction. An alternating direction implicit method is used to solve the equations in primitive variables.

For large values of the axial distance, the present calculation for the case of coplanar leading edges is in good agreement with those of previous investigators.

Key Words:

Navier-Stokes equations
Alternating direction implicit method
Incompressible flow
Viscous flow
Three-dimensional boundary layers
Axial corner

TABLE OF CONTENTS

	Page
ABSTRACT	ii
INTRODUCTION	1
SYMBOLS	3
ANALYSIS	5
Governing Differential Equations	8
Boundary Conditions	13
NUMERICAL ANALYSIS	16
ADI Method	16
Linearization Scheme	19
Boundary Conditions	20
Method (a)	20
Method (b)	22
RESULTS AND DISCUSSION	22
CONCLUDING REMARKS	28
APPENDIX A: POTENTIAL FLOW SOLUTION	32
APPENDIX B: HALF AXIAL STEP - IMPLICIT IN η DIRECTION	34
APPENDIC C: FULL AXIAL STEP - IMPLICIT IN ζ DIRECTION	35
APPENDIX D: MATRIX COEFFICIENTS OF THE LINEARIZED DIFFERENCE EQUATIONS, METHOD (a)	37
APPENDIX E: MATRIX COEFFICIENTS OF THE LINEARIZED DIFFERENCE EQUATIONS, METHOD (b)	44
REFERENCES	46

LIST OF FIGURES

Figure		Page
1	Corner flow geometry	6
2	Corner flow configuration and subdivisions	7
3	Discretized grid system and the ADI procedure	18
4	Isovels of the axial velocity	24
5	Axial velocity along symmetry line	25
6	Skin friction parameter in corner layer	26
7	Secondary velocity along symmetry line	27
8	Secondary flow vectors in the corner layer	29
9	Isobars in the corner layer	30
10	Effect of axial distance on the axial velocity	31

INVESTIGATION OF AN INCOMPRESSIBLE FLOW ALONG A CORNER BY AN ALTERNATING DIRECTION IMPLICIT METHOD

By

Dashrath K. Patel[1]

SUMMARY

The axial corner flow is analyzed for the incompressible laminar boundary layer flow. The governing equations are derived from the Navier-Stokes equations by neglecting second derivative terms of the axial direction. The complete set of governing equations is prepared in primitive variables. In this first formulation the axial pressure gradient is assumed to be zero. An alternating direction implicit method is used to solve the governing equations. For rapid convergence simultaneous solution is obtained by tridiagonal block matrices.

Results are presented for the case of coplanar leading edges in the first phase of computation. For large values of axial distance these results are in good agreement with those of previous investigators. For small values of axial distance, the present calculations indicate that the similarity concept used by previous investigators is not valid.

INTRODUCTION

The three-dimensional viscous interaction occurring in axial corners, formed along the interaction of two plane surfaces, is of fundamental interest in aerodynamic configurations such as wing-body and wing-fin junctions, wind tunnel and its support, and other applications.

The mutual interaction of the boundary layers on the two intersecting surfaces must be taken into consideration, even in the lowest order approximation

---

[1] Research Associate, Old Dominion University Research Foundation, Norfolk, Virginia 23508.

for such a flow. This makes it essential to consider the corner flow problem as a three-dimensional problem.

The early analysis of Carrier (ref. 1) for the corner flow problem has been recently improved upon by Rubin (ref. 2), who formulated it as a singular perturbation problem, including the three-dimensionality of the configuration. The method of matched asymptotic expansions was used to match systematically the corner flow to the boundary layer for large lateral distances from the corner and to the potential flow for large distances away from the walls. Pal and Rubin (ref. 3) determined the asymptotic features of the corner flow and demonstrated that consistent asymptotic series exist for the "corner layer." Further, all flow variables were found to exhibit algebraic decay into the boundary layer away from the corner; also, the crossflow velocities were shown to decay algebraically into the potential flow. Numerical solutions for the incompressible corner flow were obtained by Rubin and Grossman (ref. 4) using the Gauss Siedel method of successive iterations and by Ghia and Davis (ref. 5) using the ADI method in similarity variables.

These flows have certain characteristics which are common to boundary layer flows; for example, the velocities in the plane normal to the mainstream direction are usually much smaller than the main flow velocity. Also, one expects gradients that exist in the cross directions to be larger than the gradients in the main flow directions. Therefore, it might be reasonable to use a boundary layer scaling on the Navier-Stokes equations to effect some simplification; however, this procedure yields an inconsistent set of equations. To lowest order, the cross-stream momentum equations reduce to statements that the pressure is constant, and the resulting number of equations is not sufficient to determine the remaining unknown quantities. A set of equations which is a higher order approximation to the Navier-Stokes than the boundary layer equations, the parabolic-elliptic Navier-Stokes (PENS) equations, is necessary to overcome these difficulties.

The PENS three-dimensional equations are given in reference 6, where the leading-edge flow on a finite-width flat plate is calculated. The alternating direction implicit (ADI) method, introduced in reference 7, is used to solve the equations. The two- and three-dimensional problems are reviewed in reference 8, where a new predictor-corrector method is presented as the most appropriate one to use.

The PENS concepts have been utilized in subsonic, incompressible flow for internal (ref. 9) and external (ref. 10) cases. However, the need to solve a Poisson equation for the cross-plane pressure in these incompressible flows separates them from the procedures used in references 6 and 8.

The character of the equations is such that they are well suited to solution by the ADI method. This finite difference method generated block tridiagonal matrix equations which allow for the simultaneous solution of all the variables at each location.

This solution procedure of the PENS system is supplied to the corner layer problem. Computations are made in the cross-plane and the cross-planes are coupled by a marching procedure along the axial direction.

SYMBOLS

$a_{i,j}$	coefficients of matrix (A) in typical difference equation (37) defined in equation (40)
$b_{i,j}$	coefficients in matrix (B) defined in equation (37)
$c_{i,j}$	coefficients of matrix (C) defined in equation (37)
d_j	coefficient of vector $\vec{D}$ defined in equation (37)
$f(\eta)$	Blasius function
$g(\eta)$	function defined in equation (26)
i	axial coordinate along x for discretized problem
j	lateral coordinate along η for discretized problem
k	lateral coordinate along ζ for discretized problem
L	reference length
M	Mach number
N	value of j or k on the free stream end
P	static pressure
Q	dummy variable used for coefficients of derivatives
Re	Reynolds number
u	streamwise velocity in x direction

v	transverse velocity in y direction
w	lateral velocity in z direction
$\vec{W}$	vector of four variables (u, v, w, p), see equation (37)
x, y, z	Cartesian coordinates
Δx	step size along x direction, see equation (31)
Y	stretched transverse coordinate, defined in equation (7)
Z	stretched lateral coordinate, defined in equation (7)
β	constant defined in equation (26)
δ	total boundary layer thickness
ε_i	parameter in series expansion, defined in equation (6)
ζ	similarity coordinate in lateral direction, defined in equation (16)
$\Delta\zeta$	step size along ζ direction, defined in equation (31)
η	similarity coordinates in transverse direction, defined in equation (16)
$\Delta\eta$	step size along η direction, defined in equation (31)
λ	ratio of the consecutive step sizes defined in equation (31)
μ	shear coefficient of viscosity
ρ	density
χ	constant defined in equation (26)
ϕ	dummy variable used for u, v, w, and p

Subscripts

$0,1,2$	variables for zero, first, and second order solutions of the flow, see equation (6)
∞	free stream condition
j	denotes a grid point along η direction
k	denotes a grid point along ζ direction
max	maximum value
w	wall value

-	step size behind grid point, i, j, k, see equation (31)
+	step size ahead of grid point, i, j, k, see equation (31)

Superscripts

i	denotes a grid point along x direction
n	values of variable at iteration n, defined in equation (E-4)
*	values of the variable at the intermediate step of ADI method. Also dimensionless corner flow variables defined in series solution in equation (6).
^	dimensional flow variables in (x,y,z) coordinates
~	dimensionless flow variables in (x,y,z) coordinates
→	vector quantities
'	derivative of η or ζ

ANALYSIS

The configuration of the viscous flow along a right angle corner formed by the intersection of two equal semi-infinite flat plates is shown schematically in figure 1. Following Rubin's analysis (ref. 2), four different flow regimes are depicted. They are presented in figure 2. Region IV is primarily the region of present interest.

Formulation of the problem for region IV requires knowledge of the following flows in regions I, II, and III.

1. The zero-order potential flow in region I
2. The first-order boundary layer flow in regions II and III
3. The first-order potential flow in region I, resulting from the normal flow at the outer edges of regions II and III.
4. The second-order solution in regions II and III which is considered for crossflow velocities.

A detailed asymptotic analysis of the corner layer equations is also needed to prescribe the proper far field boundary conditions for the "corner layer" flow.

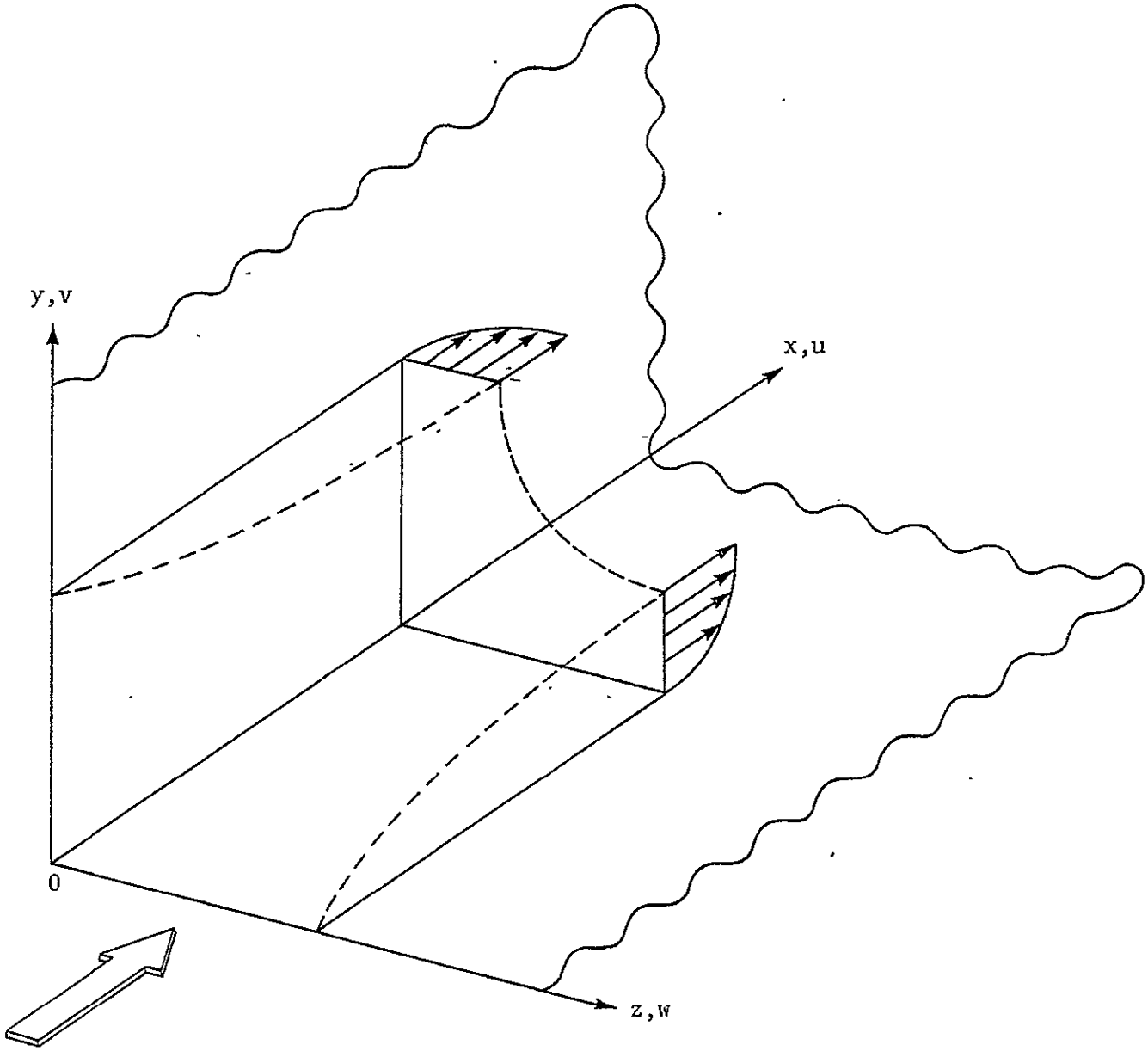

Figure 1. Corner flow geometry.

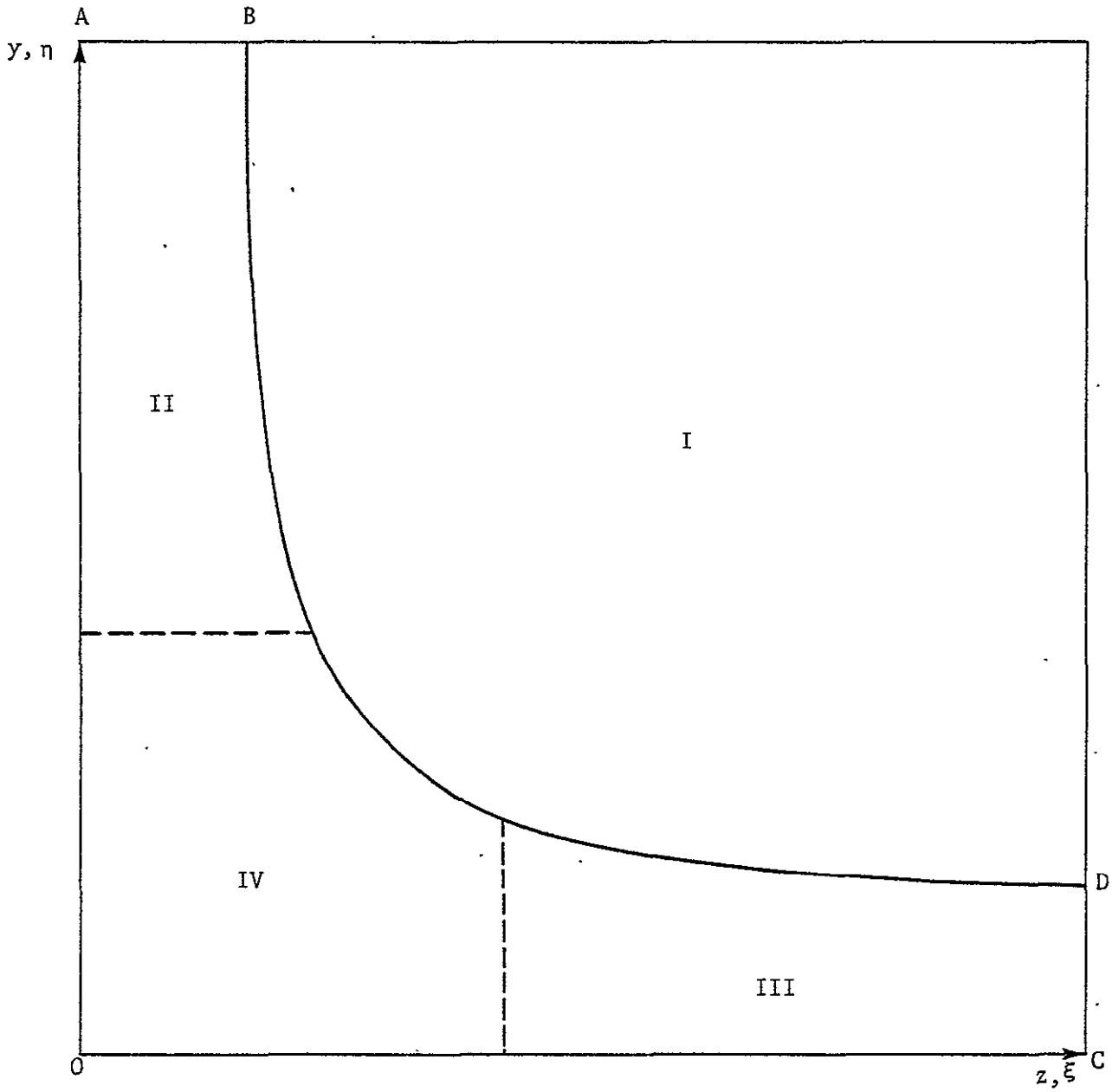

Figure 2. Corner flow configuration and subdivisions.

Region IV depicted in figure 2 is referred to as the "corner layer" flow where the flow is truly three-dimensional, because of the interaction of the boundary layers in regions II and III. The governing differential equations for this corner layer flow will now be discussed.

Governing Differential Equations

The general dimensionless Navier-Stokes equations for a viscous, incompressible steady state fluid are

Continuity

$$\frac{\partial \tilde{u}}{\partial x} + \frac{\partial \tilde{v}}{\partial y} + \frac{\partial \tilde{w}}{\partial z} = 0 \tag{1}$$

x-momentum

$$\tilde{u}\frac{\partial \tilde{u}}{\partial x} + \tilde{v}\frac{\partial \tilde{u}}{\partial y} + \tilde{w}\frac{\partial \tilde{u}}{\partial z} = -\frac{\partial \tilde{p}}{\partial x} + \frac{1}{Re}\left[\frac{\partial^2 \tilde{u}}{\partial x^2} + \frac{\partial^2 \tilde{u}}{\partial y^2} + \frac{\partial^2 \tilde{u}}{\partial z^2}\right] \tag{2}$$

y-momentum

$$\tilde{u}\frac{\partial \tilde{v}}{\partial x} + \tilde{v}\frac{\partial \tilde{v}}{\partial y} + \tilde{w}\frac{\partial \tilde{v}}{\partial z} = -\frac{\partial \tilde{p}}{\partial y} + \frac{1}{Re}\left[\frac{\partial^2 \tilde{v}}{\partial x^2} + \frac{\partial^2 \tilde{v}}{\partial y^2} + \frac{\partial^2 \tilde{v}}{\partial z^2}\right] \tag{3}$$

z-momentum

$$\tilde{u}\frac{\partial \tilde{w}}{\partial x} + \tilde{v}\frac{\partial \tilde{w}}{\partial y} + \tilde{w}\frac{\partial \tilde{w}}{\partial z} = -\frac{\partial \tilde{p}}{\partial z} + \frac{1}{Re}\left[\frac{\partial^2 \tilde{w}}{\partial x^2} + \frac{\partial^2 \tilde{w}}{\partial y^2} + \frac{\partial^2 \tilde{w}}{\partial z^2}\right] \tag{4}$$

The dimensionless variables used in the above equations are defined as follows:

$$\tilde{u} = \frac{\hat{u}}{\hat{u}_\infty} \qquad x = \frac{\hat{x}}{\hat{L}} \qquad \tilde{p} = \frac{\hat{p}}{\hat{\rho}_\infty \hat{u}_\infty^2}$$

$$\tilde{v} = \frac{\hat{v}}{\hat{u}_\infty} \qquad y = \frac{\hat{x}}{\hat{L}} \qquad Re = \frac{\hat{\rho}_\infty \hat{u}_\infty \hat{L}}{\hat{\mu}} \tag{5}$$

$$\tilde{w} = \frac{\hat{w}}{\hat{u}_\infty} \qquad z = \frac{\hat{z}}{\hat{L}}$$

Now the corner layer flow solution is considered as the first term in a series expansion, for the solution of the complete Navier-Stokes equations, using some appropriate small parameters ε_i. Therefore, the variables in equations (1) to (4) are represented by the following series:

$$\begin{aligned}
\tilde{u} &= u_0^* + \varepsilon_1 u_1^* + \varepsilon_2 u_2^* + \ldots \\
\tilde{v} &= v_0^* + \varepsilon_1 v_1^* + \varepsilon_2 v_2^* + \ldots \\
\tilde{w} &= w_0^* + \varepsilon_1 w_1^* + \varepsilon_2 w_2^* + \ldots \\
\tilde{p} &= p_0^* + \varepsilon_1 p_1^* + \varepsilon_2 p_2^* + \ldots
\end{aligned} \tag{6}$$

where ε_1, ε_2 ... are the parameters of the series and $\varepsilon_2 << \varepsilon_1 << 1$ and so on (see ref. 11).

As discussed in the introduction, the cross velocities are usually much smaller than the main flow velocity. Therefore, a boundary layer scaling is taken into account, and v_0^* amd w_0^* are assumed zero in equation (6).

With the boundary layer concept the independent lateral variables for the corner layer are stretched without change of axial length x as follows:

$$Y = y\, Re^{1/2} \qquad \text{and} \qquad Z = z\, Re^{1/2} \tag{7}$$

Further, in equation (6) v_0^* and W_0^* are zero and thus $\tilde{v}$ and $\tilde{W}$ are of order ε_1 in equation (6). From the continuity equation it can be shown that

$$\varepsilon_1 = Re^{-1/2} \tag{8}$$

With consideration of the power series, it is assumed that

$$\varepsilon_2 = \varepsilon_1^2 = Re^{-1} \tag{9}$$

This assumption is appropriate to obtain the governing equations by retaining the lowest order terms of the Navier-Stokes equations [eqs. (1) to (4)]. Thus, the following equations result:

Continuity

$$\frac{\partial u_0^*}{\partial x} + \frac{\partial v_1^*}{\partial Y} + \frac{\partial w_1^*}{\partial Z} = 0 \tag{10}$$

x-momentum

$$u_0^* \frac{\partial u_0^*}{\partial x} + v_1^* \frac{\partial u_0^*}{\partial Y} + w_1^* \frac{\partial u_0^*}{\partial Z} = - \frac{\partial p_0^*}{\partial x} + \frac{\partial^2 u_o^*}{\partial Y^2} + \frac{\partial^2 u_0^*}{\partial Z^2} \tag{11}$$

Y-momentum

$$\frac{\partial p_0^*}{\partial Y} = 0 \qquad \frac{\partial p_1^*}{\partial Y} = 0 \tag{12}$$

$$u_0^* \frac{\partial v_1^*}{\partial x} + v_1^* \frac{\partial v_1^*}{\partial Y} + w_1^* \frac{\partial v_1^*}{\partial Z} = - \frac{\partial p_2^*}{\partial Y} + \frac{\partial^2 v_1^*}{\partial Y^2} + \frac{\partial^2 v_1^*}{\partial Z^2} \tag{13}$$

Z-momentum

$$\frac{\partial p_0^*}{\partial Z} = 0 \qquad \frac{\partial p_1^*}{\partial Z} = 0 \tag{14}$$

$$u_0^* \frac{\partial w_1^*}{\partial x} + v_1^* \frac{\partial w_1^*}{\partial Y} + w_1^* \frac{\partial w_1^*}{\partial Z} = - \frac{\partial p_2^*}{\partial Z} + \frac{\partial^2 w_1^*}{\partial Y^2} + \frac{\partial^2 w_1^*}{\partial Z^2} \tag{15}$$

Near the leading edge, the normal velocity is very large. Thus, the solution near the leading edge is singular in these variables. Therefore, to get the finite value of v and w near the leading edges, a transformation is applied to equations (10) to (15). To get more details of the flow near the leading edge region, using a uniform or a variable grid in the computational plane, the lateral independent variables are also transformed. The system in (x,Y,Z) coordinates is transformed to (x,η,ζ) coordinates as follows:

$$\begin{aligned} u(x,\eta,\zeta) &= u_0^*(x,Y,Z) \\ v(x,\eta,\zeta) &= \sqrt{2X}\, v_1^*(x,Y,Z) \\ w(x,\eta,\zeta) &= \sqrt{2X}\, w_1^*(x,Y,Z) \\ p(x,\eta,\zeta) &= p_2^*(x,Y,Z) \end{aligned} \tag{16}$$

where

$$\eta = \frac{Y}{\sqrt{2x}} \qquad \zeta = \frac{Z}{\sqrt{2x}}$$

The governing differential equations for the corner layer in terms of the new coordinates (x,η,ζ), and the new dependent variables are written:

Continuity

$$2x\frac{\partial u}{\partial x} - \left(\eta\frac{\partial u}{\partial \eta} - \frac{\partial v}{\partial \eta}\right) - \left(\zeta\frac{\partial u}{\partial \zeta} - \frac{\partial w}{\partial \zeta}\right) = 0 \tag{17}$$

X-momentum

$$2x\,u\frac{\partial u}{\partial x} - (u\eta - v)\frac{\partial u}{\partial \eta} - (u\zeta - w)\frac{\partial u}{\partial \zeta} = \frac{\partial^2 u}{\partial \eta^2} + \frac{\partial^2 u}{\partial \zeta^2} \tag{18}$$

η-momentum

$$2x\,u\frac{\partial v}{\partial x} - (u\eta - v)\frac{\partial v}{\partial \eta} - (u\zeta - w)\frac{\partial v}{\partial \zeta} - uv = -2x\frac{\partial p}{\partial \eta} + \frac{\partial^2 v}{\partial \eta^2} + \frac{\partial^2 v}{\partial \zeta^2} \tag{19}$$

ζ-momentum

$$2x\,u\frac{\partial w}{\partial x} - (u\eta - v)\frac{\partial w}{\partial \eta} - (u\zeta - w)\frac{\partial w}{\partial \zeta} - uw = -2x\frac{\partial p}{\partial \zeta} + \frac{\partial^2 w}{\partial \eta^2} + \frac{\partial^2 w}{\partial \zeta^2} \tag{20}$$

There are four unknown variables, u, v, w, and p, and there are four governing equations. Thus, a solution is possible. But, pressure p appears only in first derivative and there is no p term in the continuity equation. Therefore, a numerical computation will create instability. To resolve this problem, a separate Poisson type pressure equation is derived as follows. The x-momentum equation is differentiated along x, the η-momentum equation is differentiated along η, the ζ-momentum equation is differentiated along ζ, and then all three equations are added. With the help of the continuity equation, the resulting equation is simplified, and finally the pressure equation is obtained as follows:

$$\frac{\partial^2 p}{\partial \eta^2} + \frac{\partial^2 p}{\partial \zeta^2} = \frac{1}{x}\left\{\left(2\dot{x}\,\frac{\partial u}{\partial x} - \eta\,\frac{\partial u}{\partial \eta} - \zeta\,\frac{\partial u}{\partial \zeta}\right)\left(\frac{\partial v}{\partial \eta} + \frac{\partial w}{\partial \zeta}\right)\right.$$

$$+ \frac{\partial v}{\partial \eta}\frac{\partial w}{\partial \zeta} - \frac{\partial v}{\partial \zeta}\frac{\partial w}{\partial \eta} - \frac{\partial u}{\partial \eta}\left(2x\,\frac{\partial v}{\partial x} - \eta\,\frac{\partial v}{\partial \eta} - \zeta\,\frac{\partial v}{\partial \zeta} - v\right) \tag{21}$$

$$\left. - \frac{\partial u}{\partial \zeta}\left(2x\,\frac{\partial w}{\partial x} - \eta\,\frac{\partial w}{\partial \eta} - \zeta\,\frac{\partial w}{\partial \zeta} - w\right)\right\}.$$

Thus, the final form of the differential equations governing the corner layer flow is given by equations (18) through (21).

Boundary Conditions

As the flow equations (18) to (20) are of the PENS type and equation (21) is of the elliptic type in the cross plane (η,ζ), the boundary conditions are required on all boundaries of a closed region in the (η,ζ) plane. The boundary conditions along the plate surfaces $\eta = 0$, $\zeta = 0$ are taken similar to no-slip boundary layer flow.

On the far field boundary from the corner (in the boundary layer region), the asymptotic analysis of the corner layer equations provides the necessary boundary conditions. For the solution of corner flow within a finite computational domain, the boundary conditions as provided by Pal and Rubin (ref. 3) or Ghia and Davis (ref. 5) will be used. The complete boundary conditions used for the domain are given below.

At the plate surface, $\eta = 0$ (along OC in figure 2)

$$u(0,\zeta) = 0, \quad v(0,\zeta) = 0, \quad w(0,\zeta) = 0 \tag{22}$$

and

$$\frac{\partial p}{\partial \eta}(0,\zeta) = 0$$

At the plate surface, $\zeta = 0$ (along OA in figure 2)

$$u(\eta,0) = 0, \quad v(\eta,0) = 0, \quad w(\eta,0) = 0 \tag{23}$$

and

$$\frac{\partial p}{\partial \zeta}(\eta,0) = 0$$

At the far field boundary, the boundary conditions in boundary layer region and in inviscid region are separately provided. It was assumed that boundary layer edge occurs when $\frac{u}{u_\infty}$ reaches a value of 0.99.

At the far field boundary, within the boundary layer region at $\zeta = \zeta_{max}$ and for all η (along CD in figure 2):

$$\begin{aligned} u(\eta,\zeta) &= f'(\eta) + x\,\eta\, f''(\eta)\,\zeta^{-2} \\ v(\eta,\zeta) &= [\eta\, f'(\eta) - f(\eta)] \\ &\quad - \chi[-\eta^2 f''(\eta) + 3\eta\, f'(\eta) + f(\eta)]\zeta^{-2} \\ w(\eta,\zeta) &= \beta\, g(\eta) - 4\chi\, f'(\eta)\zeta^{-1} \end{aligned} \tag{24}$$

and at $\eta = \eta_{max}$ and for all ζ (along AB in figure 2)

$$\begin{aligned} u(\eta,\zeta) &= f'(\zeta) + x\,\zeta\, f''(\zeta)\eta^{-2} \\ w(\eta,\zeta) &= [\zeta\, f'(\zeta) - f(\zeta)] \\ &\quad - \chi[-\zeta^2 f''(\zeta) + 3\zeta\, f'(\zeta) + f(\zeta)]\eta^{-2} \\ v(\eta,\zeta) &= \beta\, g(\zeta) - 4\chi\, f'(\zeta)\eta^{-1} \end{aligned} \tag{25}$$

where

$f(\eta)$ is the Blasius function

$$\chi = -2.5$$

$$\beta = \lim_{\eta \to \infty} [\eta - f(\eta)] = 1.21678 \tag{26}$$

$$g(\eta) = f''(\eta) \int_0^{\eta} \frac{\tau - \beta}{f''(\tau)} \, d\tau$$

To calculate the boundary conditions for the inviscid corner region, the first-order potential flow solution in the region IV is essential. The solution for three velocity components is shown as follows:

$$u = 1 - \frac{\beta}{Re\sqrt{2}} \left[\frac{\eta \left(x + \frac{2\eta^2}{Re} \right)^{-1/2}}{\left(x + \sqrt{x^2 + \frac{2\eta^2}{Re} x} \right)^{1/2}} \right]$$

$$- \frac{\beta}{Re\sqrt{2}} \left[\frac{\zeta \left(x + \frac{2\zeta^2}{Re} \right)^{-1/2}}{\left(x + \sqrt{x^2 + \frac{2\zeta^2}{Re} x} \right)^{1/2}} \right] \tag{27}$$

$$v = \frac{\beta}{\sqrt{2}} \left[\frac{x + \sqrt{x^2 + \frac{2\eta^2}{Re} x}}{x + \frac{2\eta^2}{Re}} \right]^{1/2} \tag{28}$$

$$w = \frac{\beta}{\sqrt{2}} \left[\frac{x + \sqrt{x^2 + \frac{2\zeta^2}{Re} x}}{x + \frac{2\zeta^2}{Re}} \right]^{1/2} \tag{29}$$

The derivation and details of the above equations are represented in Appendix A. The pressure is calculated by the use of the Bernoulli's equation. The expression for pressure calculation is given as follows:

$$p = p_\infty + \frac{1}{2}\left\{(u_\infty^2 - u^2) - \frac{v^2 + w^2}{2Re\ x}\right\} \tag{30}$$

In the boundary layer region (along AB and CD in figure 2), the presure is assumed constant.

The mathematical model for the corner layer flow is now complete. The solution of these nonlinear coupled partial differential equations [eqs. (18) to (21)], subject to the boundary conditions given in equations (22) to (30), is obtained numerically using the ADI method. The details of the numerical analysis are presented in the next section.

NUMERICAL ANALYSIS

ADI Method

Although explicit difference schemes are conceptually less complex and thus more easily coded than implicit methods, explicit finite difference methods are restricted to small axial distance steps relative to the spatial grid size for numerical stability. Consequently, explicit methods generally require a large total computation time to reach a steady state flow condition. On the other hand, most implicit methods are found to be unconditionally stable in linearized stability analyses for model equations similar to the Navier-Stokes equations. Therefore, it is expected that implicit methods will allow larger axial steps than explicit methods when applied to the Navier-Stokes equations.

The ADI technique developed by Peaceman and Rachford (ref. 7) was used in the present study. This ADI method is a two-step procedure requiring reduction of tridiagonal matrices for which an efficient solution algorithm, the Thomas algorithm, exists. Roach (ref. 12) states that ADI methods are currently the most popular approach to computing incompressible viscous Navier-Stokes flows. He notes that although these methods have not been found to be unconditionally stable in practice, the somewhat larger axial steps obtainable have resulted in faster overall computation times by a factor of two or more.

The ADI procedure is a two-step, second-order accurate implicit integration technique. The first step advances the solution from the location (i) to an intermediate stage of computation (i+1/2), much like a predictor step j, and the second step advances the solution to the new location (i+1), much like a corrector step. The solution generated is then second order accurate about the point (i+1).

Two types of approaches are taken for obtaining the solutions of the governing equations (18) to (21):

a. In the first method all four governing equations are solved simultaneously by the ADI method;

b. In the second method three momentum equations [eqs. (18) to (20)] are solved simultaneously by the ADI method, and the Poisson-type pressure equation is solved by the Gauss-Siedel (explicit) method.

A variable grid system is adopted for the finite difference formulation. It is shown in figure 3. The superscript i is taken along axial direction x; the subscript j is taken along the η direction; and the subscript k is taken along the ζ direction. The ratio of consecutive grid spacing along any axis is kept constant, i.e.,

$$\frac{\Delta x_+}{\Delta x_-} = \frac{x^{i+1} - x^i}{x^i - x^{i-1}} = \lambda$$

$$\frac{\Delta \eta_+}{\Delta \eta_-} = \frac{\eta_{j+1} - \eta_j}{\eta_j - \eta_{j-1}} = \lambda \qquad (31)$$

$$\frac{\Delta \zeta_+}{\Delta \zeta_-} = \frac{\zeta_{k+1} - \zeta_k}{\zeta_k - \zeta_{k-1}} = \lambda$$

In the variable grid system the derivatives of any dependent variable ϕ are written in finite difference form as follows:

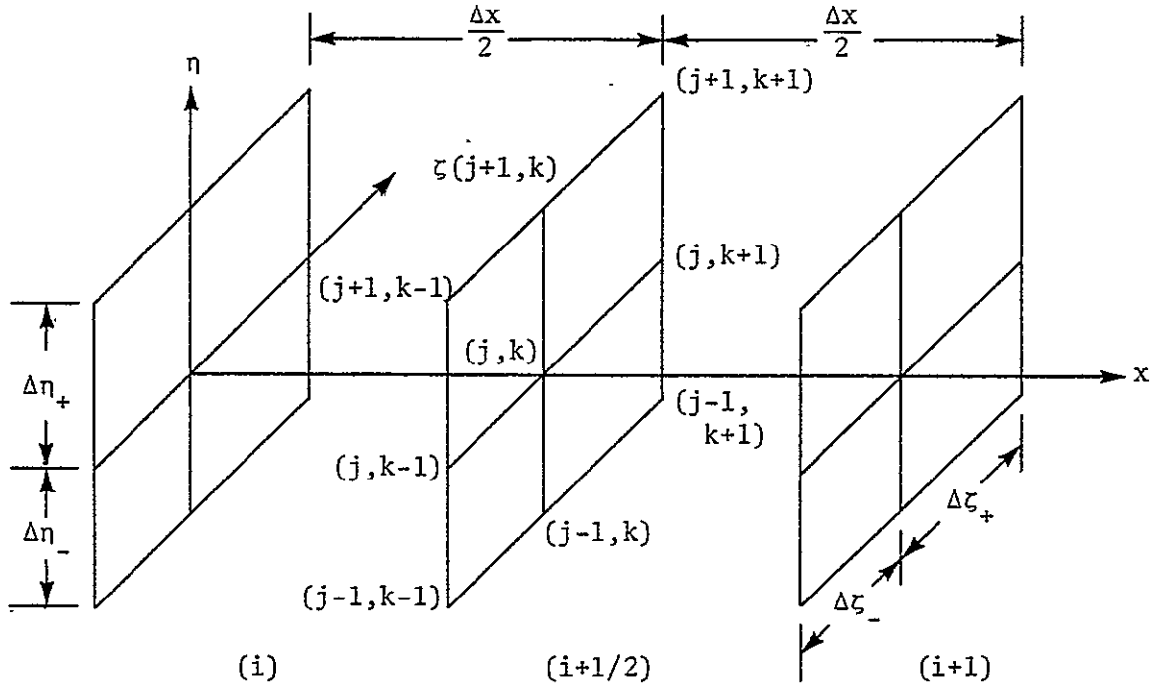

Figure 3. Discretized grid system and the ADI procedure.

$$\left.\frac{\partial\phi}{\partial\eta}\right|_{j,k} = \frac{\Delta\eta_-^2\,\phi_{j+1,k} - \Delta\eta_+^2\,\phi_{j-1,k} + (\Delta\eta_+^2 - \Delta\eta_-^2)\phi_{j,k}}{\Delta\eta_+\,\Delta\eta_-\,(\Delta\eta_+ + \Delta\eta_-)}$$

$$- \frac{\Delta\eta_+\,\Delta\eta_-}{6}\left.\frac{\partial^3\phi}{\partial\eta^3}\right|_{j,k} + O(\Delta\eta^3) \tag{32}$$

$$\left.\frac{\partial^2\phi}{\partial\eta^2}\right|_{j,k} = \frac{\Delta\eta_-\,\phi_{j+1,k} - (\Delta\eta_+ + \Delta\eta_-)\phi_{j,k} + \Delta\eta_+\,\phi_{j-1,k}}{\frac{\Delta\eta_+\,\Delta\eta_-}{2}\,(\Delta\eta_+ + \Delta\eta_-)}$$

$$- \left(\frac{\Delta\eta_+ - \Delta\eta_-}{3}\right)\left.\frac{\partial^3\phi}{\partial\eta^3}\right|_{j,k} + O(\Delta\eta^2) \tag{33}$$

A similar technique is used for the finite difference forms of $\frac{\partial\phi}{\partial\zeta}$ and $\frac{\partial^2\phi}{\partial\zeta^2}$.

Linearization Scheme

The ADI method is actually formulated for only linear equations. But the governing equations are nonlinear. Thus, a method must be developed to compute all the nonlinear coefficients (and the derivatives in the pressure equation). This linearization can be accomplished by a quadratic extrapolation from the two previous x-stations i and (i-1). All of these nonlinear coefficients and derivatives are calculated at the (i+1/2) point by extrapolation using

$$Q_{j,k}^{i+1/2} = \frac{\left(\frac{1}{2}\,\Delta x_+ + \Delta x_-\right)Q_{j,k}^{i} - \frac{1}{2}\,\Delta x_+\,Q_{j,k}^{i-1}}{\Delta x_-} \tag{34}$$

where Q refers to any of these quantities needed for extrapolation.

Boundary Conditions

Boundary conditions of velocity components are very simple and are discussed in the previous section. Boundary conditions for pressure are taken as $\frac{\partial p}{\partial \eta}$ or $\frac{\partial p}{\partial \zeta}$ and are zero. In finite difference form to satisfy the above condition wall pressure p_1 is denoted in terms of p_2 and p_3 by

$$p_w = p_1 = \frac{(1 + \lambda)^2 p_2 - p_3}{\lambda(\lambda + 2)} \tag{35}$$

On the far field free boundaries the boundary conditions of all four variables are given during first iteration by equations (24) to (30). After first iteration, the boundary condition of all four variables is changed to

$$\frac{\partial^2 \phi}{\partial \eta^2} = 0 \quad \text{For } \eta \text{ direction}$$

and

$$\frac{\partial^2 \phi}{\partial \zeta^2} = 0 \quad \text{For } \zeta \text{ direction}$$

where ϕ is one of the variables u, v, w, p. Using finite difference formulation end value ϕ_N is calculated in terms ϕ_{N-1} and ϕ_{N-2} by

$$\phi_N = (1 + \lambda)\phi_{N-1} - \lambda \phi_{N-2} \tag{36}$$

Method (a)

By using the extrapolation [eq. (33)] for the nonlinear coefficients and derivatives in equations (18) to (21), the ADI difference approximation for these equations results in a linear set of four equations in four unknowns at each step of the marching procedure. A set of equations for the first half axial step and implicit in the η direction is given in Appendix B. A set of equations for the full axial step and implicit in the ζ direction is given in Appendix C.

For a more efficient approach to getting a solution, the four equations are coupled and solved simultaneously. The method is quite advantageous because, in addition to eliminating the choice of solution order, it makes more sense by allowing changes in any variable to be instantaneously sensed by all others.

Let $\vec{W}_k = (u,v,w,p)$ be an unknown vector which contains four variables. For the sweep of the ADI procedure, where ζ-derivatives are differenced implicitly along one line of the ζ direction, the resulting matrix equation derived from governing equations (18) to (21) has a block tridiagonal structure as shown below.

$$[A]_k \vec{W}_{k-1} + [B]_k \vec{W}_k + [C]_k \vec{W}_{k+1} = \vec{D}_j \tag{37}$$

where

$$\vec{W}_k = (u,v,w,p) \tag{38}$$

and $\vec{D}_j$ is a known source term vector along the η direction,

$$\vec{D}_j = (d_1, d_2, d_3, d_4)_j \tag{39}$$

The coefficients (A), (B), and (C) are block matrices of size 4×4, for example:

$$[A]_k = \begin{bmatrix} a_{11} & a_{12} & a_{13} & a_{14} \\ a_{21} & a_{22} & a_{23} & a_{24} \\ a_{31} & a_{32} & a_{33} & a_{34} \\ a_{41} & a_{42} & a_{43} & a_{44} \end{bmatrix}_k \tag{40}$$

The components a_{mn} represent of the nth unknown variable from the mth equation at point k. The coefficients $(A)_k$, $(B)_k$, and $(C)_k$ are given in Appendix D.

The inversion of this block matrix is obtained by standard procedure, (ref. 13).

Method (b)

In this approach, instead of all four equations, three momentum equations are solved simultaneously with known values for pressure as calculated at station (i+1/2) by extrapolation of data from stations i and (i-1). After the first iteration the new calculated pressure data of station (i+1/2) is used, obtained by interpolation of calculated pressure of station (i+1) and of known pressure of station i.

During the first half axial step march equations (B-1) to (B-3) from Appendix B are used, and during the next half axial step march the equations (C-1) to (C-3) from Appendix C are used. In this computation, the tridiagonal block matrices are of order 3 × 3 and the vector $\vec{W} = (u,v,w,)$. The coefficients of the matrices A, B, and C, and of source vector D are shown in Appendix E.

The pressure equation has no x derivative as the gradient of pressure along the axial direction is neglected. Thus, the pressure equation is an elliptic equation. Therefore, it is convenient to solve the pressure equation by the Gauss-Siedel method.

RESULTS AND DISCUSSION

In the first phase of the computation, uniform space grid system ($\lambda = 1$) is adopted along the x, η, and ζ directions; 51 × 51 grid points are taken in the computation cross plane; η_{max} as well as ζ_{max} are taken of the same magnitude and equal to 9. Thus, in the uniform space grid system, each grid space is of 0.18 × 0.18 size. The variables u, v, w, and p are calculated in the cross plane by providing the appropriate boundary conditions. In method (a), for better convergence, 5 to 10 iterations are adopted with the ADI method in each cross plane calculation. During the first iteration the coefficients of the nonlinear derivatives are extrapolated at the (i+1/2) location by the known values of i and (i-1) locations, by equation (34). Later the nonlinear coefficients are calculated at (i+1/2) location by interpolation by the known values of i location and the latest computer values of (i+1) location. Near the leading edge 10 iterations are adopted, and in the downstream part 5 iterations are considered. Some oscillations of the result are observed near the leading edge computation. In downstream marching, the oscillations are damped out. In the downstream section the result is observed

converged even in 5 iterations. In method (b) pressure equation (21) is solved by the Gauss-Siedel (explicit) method, thus for each iteration of ADI method 20 iterations are given to the pressure equation. These are sufficient to obtain a converged solution. With both methods computation is carried out for a Reynolds number of 1000 and a Mach number 0.02. The results by both methods are almost identical. There is some deviation in pressure data. The governing equations are completely independent of the value of the Reynolds number.

Figure 4 depicts isovels of the axial velocity u in the cross plane, $\eta o \zeta$. The results found by Rubin and Grossman (ref. 4) are also plotted in the figure. Their result is obtained from similarity variables, and it is valid for any location along the axial direction. But in the present method the computation is carried out marching along the axial direction. The result plotted is for large values of axial distance. The isovels of the present result are very close to the isovels of Rubin and Grossman. The present result is in good agreement with their result. The result indicates that the boundary layer thickness δ on the planes $\eta = 0$ and $\zeta = 0$ toward the corner layer and both the perpendicular boundary layers merge to a single boundary layer by a smooth curvature. More details about the characteristics of the axial velocity are discussed in references 2 to 5. Thus, the discussion about the axial velocity is not given here.

Axial velocity u along the symmetry line is plotted in figure 5. The plot reveals that in the corner layer, due to the growth of the crossflow, there is a decrement of the axial velocity.

The skin friction parameter $\frac{\partial u}{\partial \eta}$ at $\eta = 0$ is plotted along the ζ direction in figure 6. The skin friction coefficient is defined by

$$c_f = \left(\frac{2\nu}{U_\infty x}\right)^{1/2} \left.\frac{\partial u}{\partial \eta}\right|_{\eta=0}$$

as shown in figure 6. The skin friction parameter is zero at the corner and increases monotonically to its asymptotic two-dimensional value of 0.4696. This result is compared with the result of Rubin and Grossman, and the present result is in good agreement with their result.

The lateral velocity w along the symmetry line is plotted in figure 7. The velocity w increases rapidly in the corner region to a maximum value at

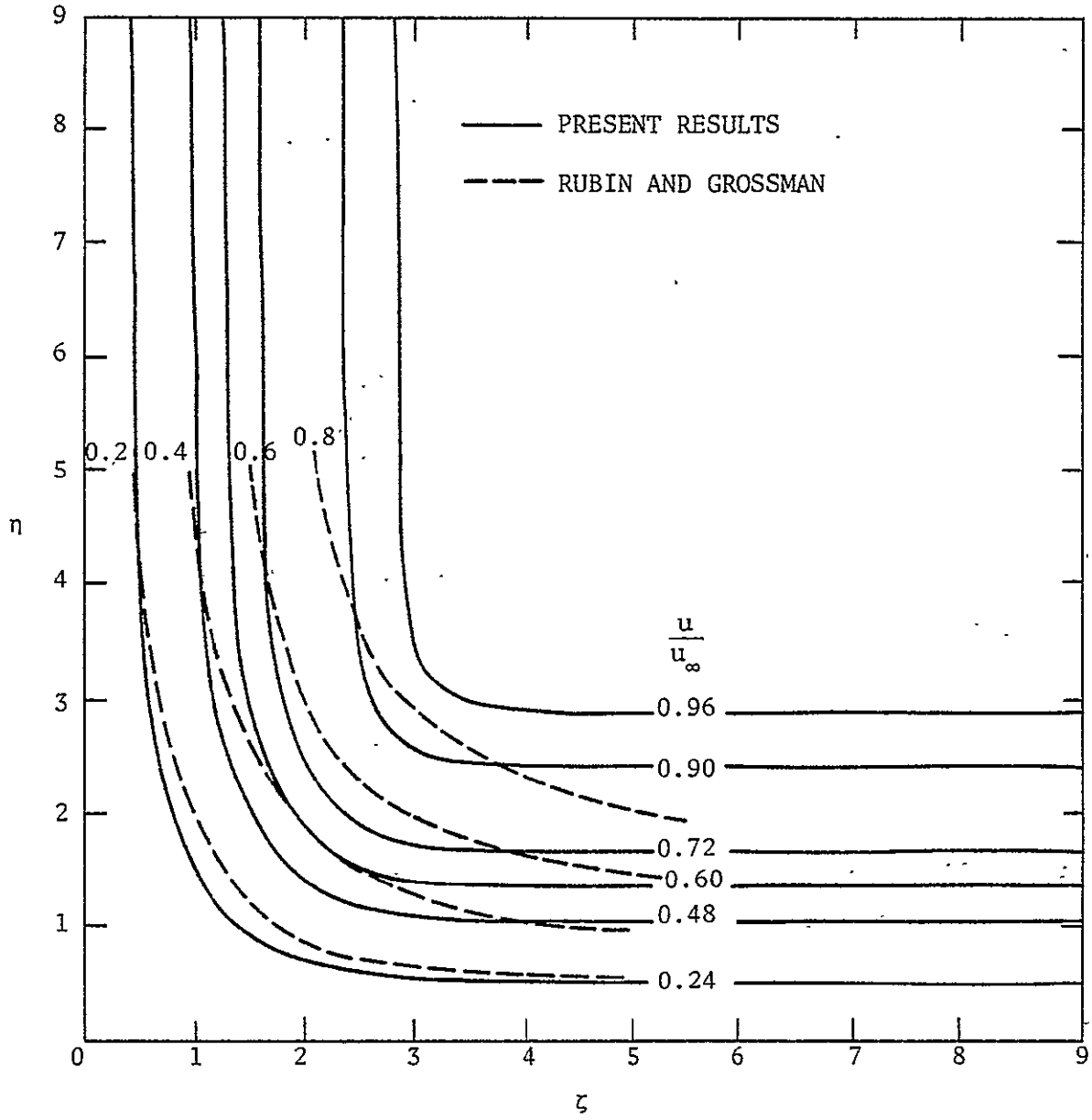

Figure 4. Isovels of the axial velocity.

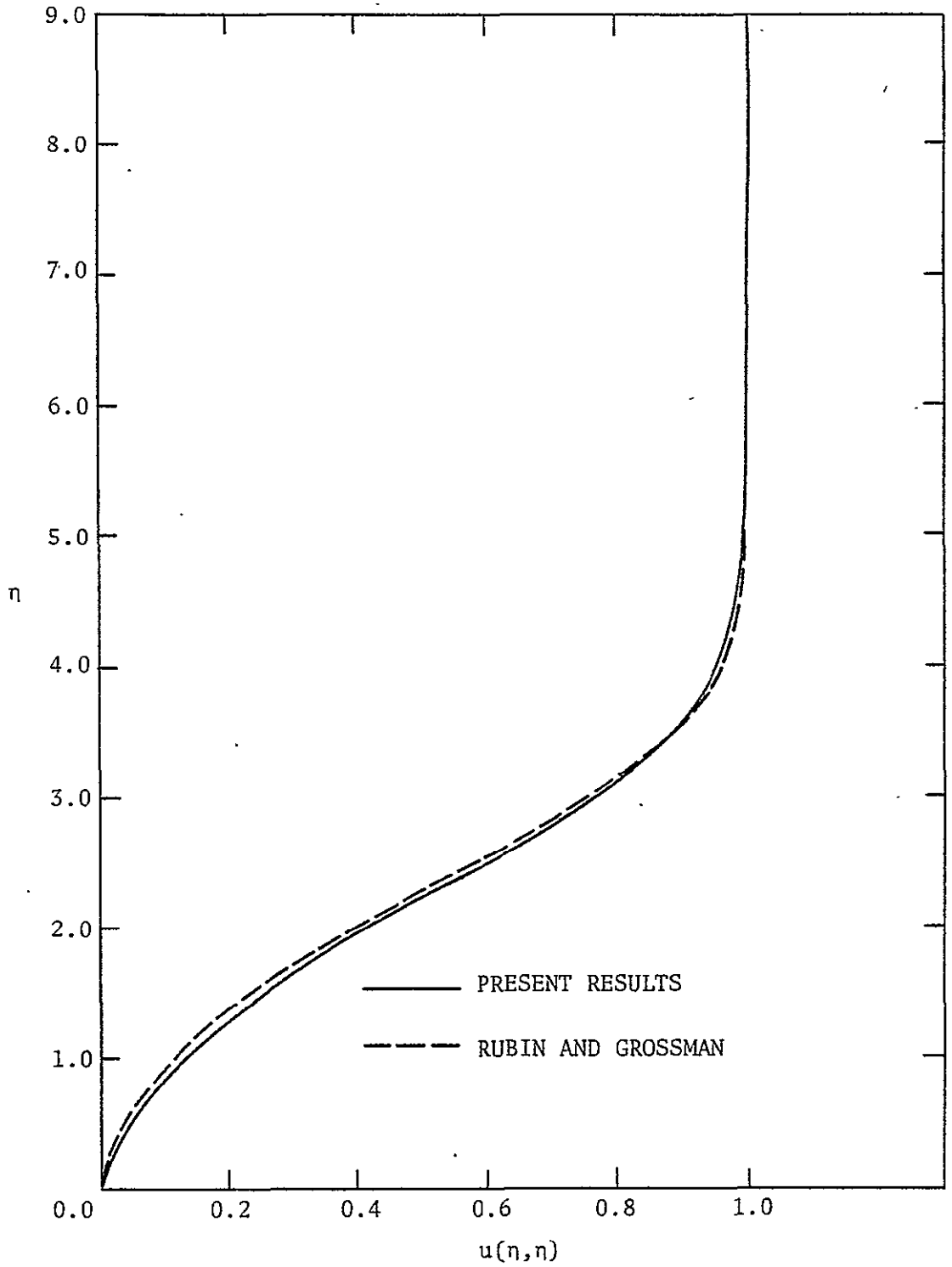

Figure 5. Axial velocity along symmetry line.

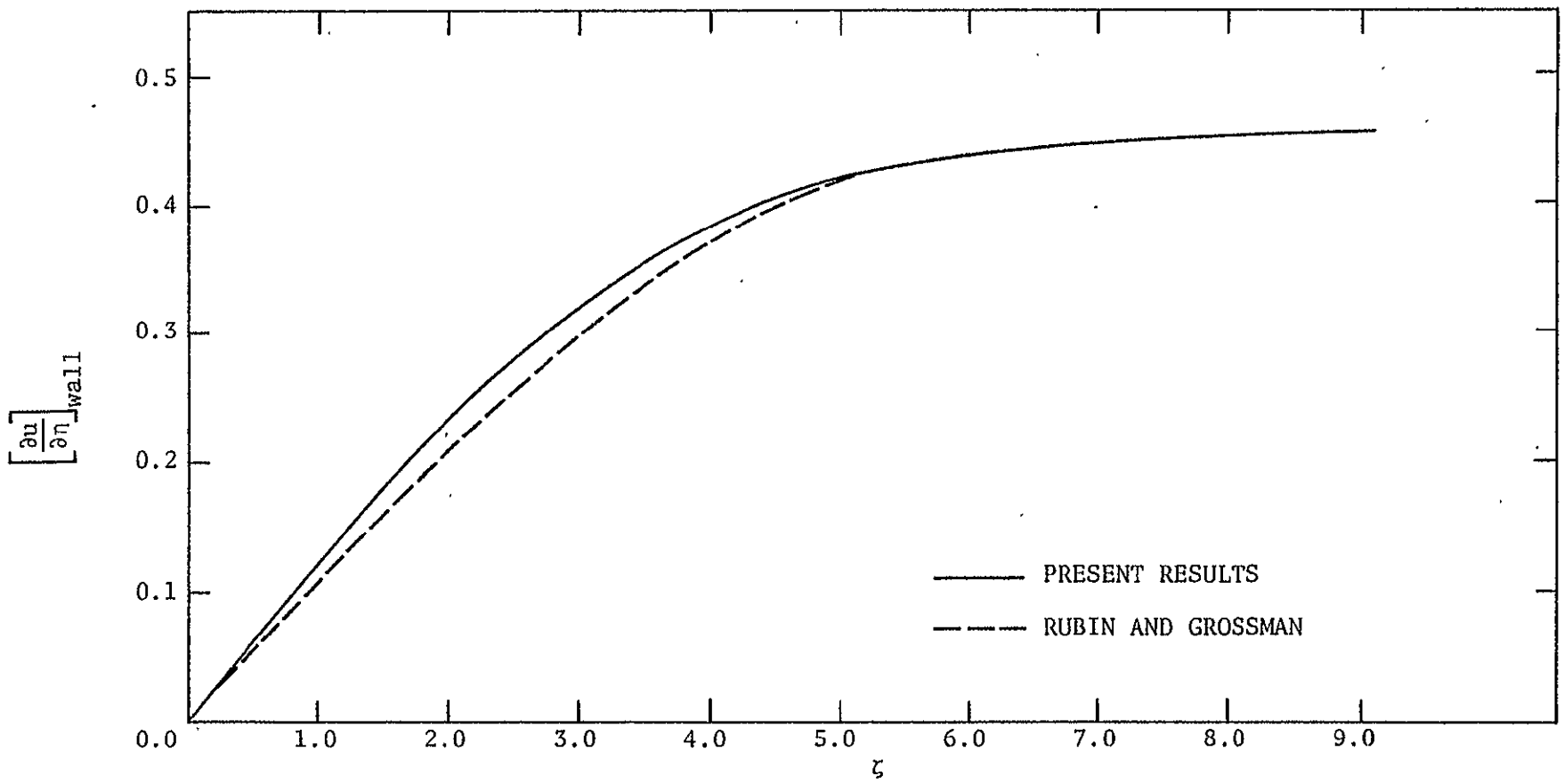

Figure 6. Skin friction parameter in corner layer.

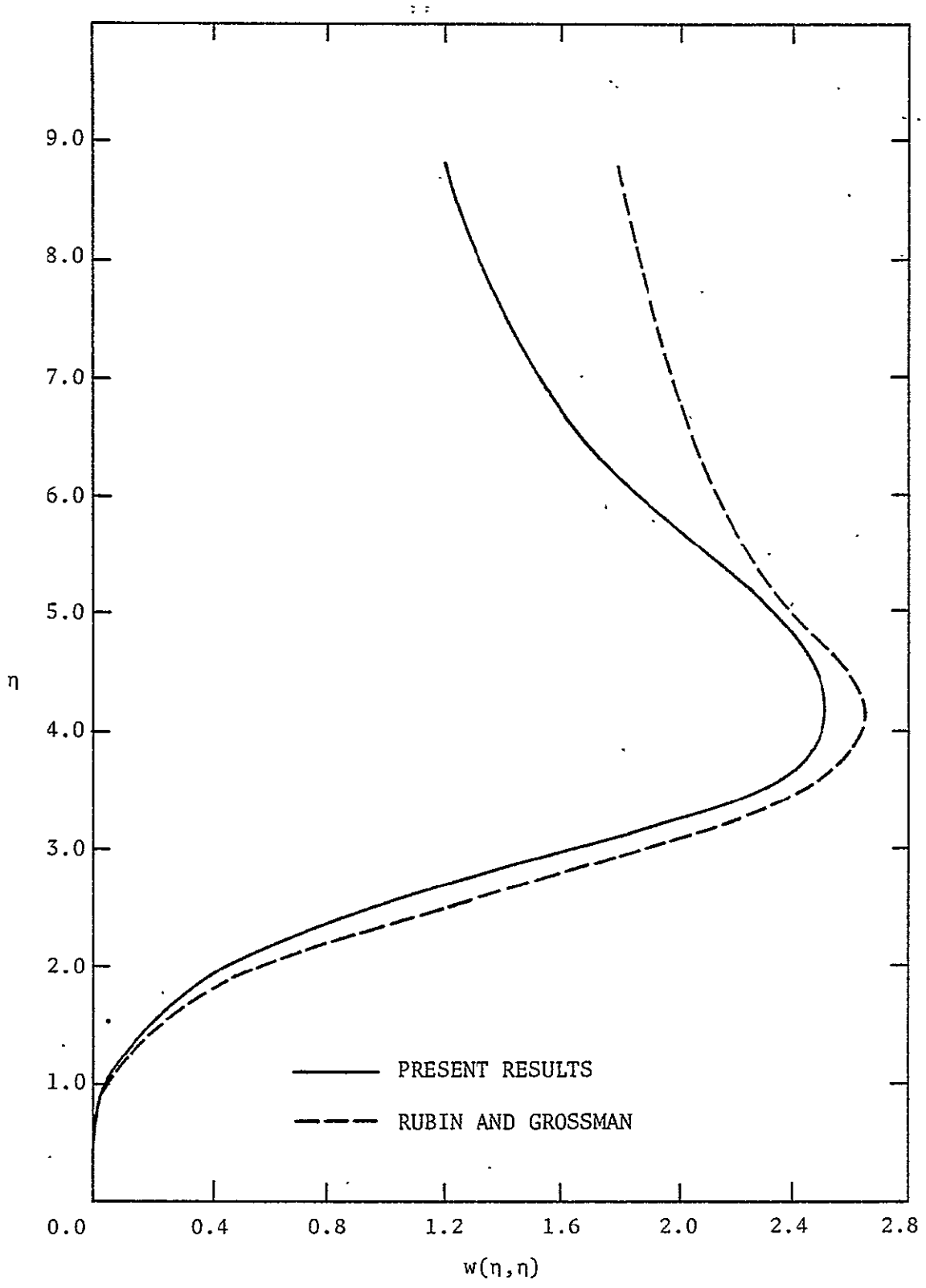

Figure 7. Secondary velocity along symmetry line.

the edge of the boundary layer. In the potential flow region this velocity decays algebraically toward the value of zero. It is observed that cross velocities near the leading edge are very small. The crossflow velocities, however, increase with increased axial distance, i.e., a secondary flow develops. This crossflow effect is of a significant amount (although constant) in the downstream portion of the corner.

The secondary crossflow vectors are plotted in figure 8. The traces inside the corner layer are drawn towards the corner line. These suggest the presence of the transverse flow along the corner walls which is towards the corner line; i.e., outflow from the corner. This plot also predicts the presence of vortices on both sides of the symmetry line, but the vortices are zero along the symmetry line.

The pressure contours are plotted in figure 9. Within the corner layer pressure is almost constant. Near the boundary layer edge the pressure decreases rapidly and reaches the minimum value. Then again, pressure rises slightly in the potential flow region. The results obtained by method (a) and method (b) are compared in this figure. The results are not in complete agreement at all grid points.

In figure 10 the effect of the axial distance on axial velocity is shown. The axial velocity along the symmetry line is plotted at different values of x location. The changes in the axial velocities are noted as the axial distance x is increased. This plot indicates that similarity solution is valid only for large values of axial distance.

CONCLUDING REMARKS

The flow along a corner formed by the intersection of two perpendicular flat plates leads to a three-dimensional boundary layer problem.

It is concluded that the similarity solution is indeed valid, but only in the downstream section. This solution, however, is not valid near the leading edge.

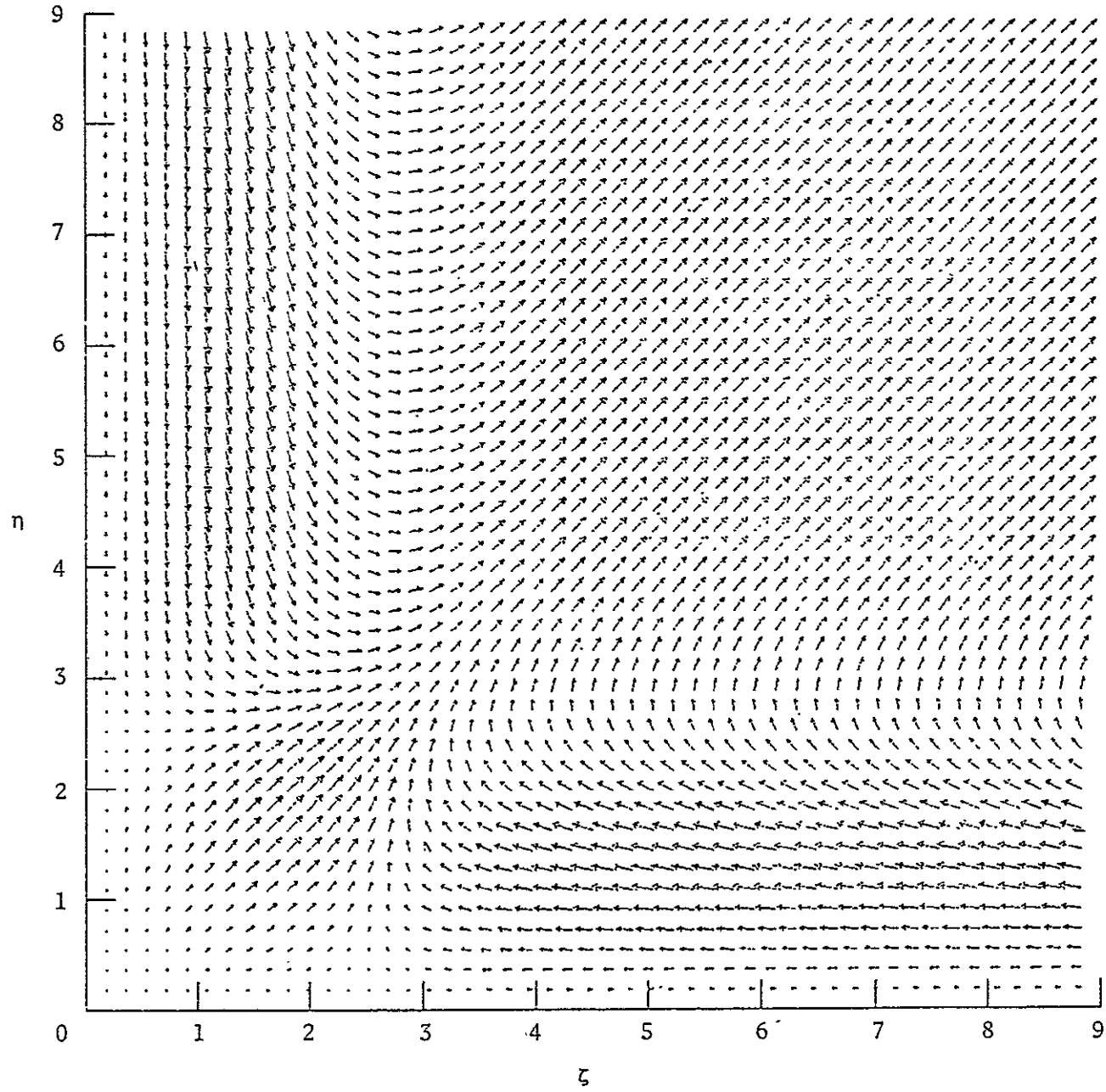

Figure 8. Secondary flow vectors in the corner layer.

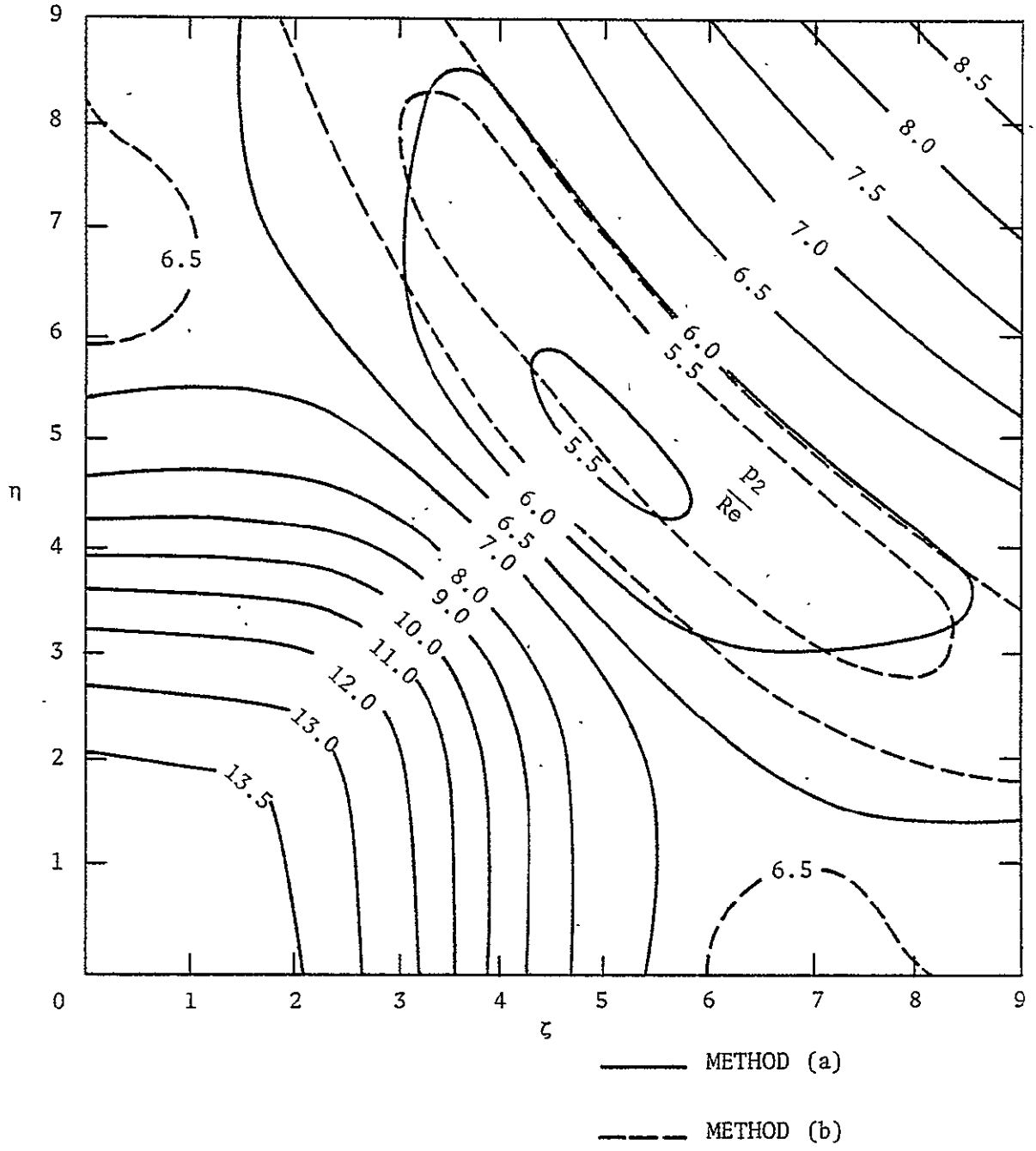

Figure 9. Isobars in the corner layer.

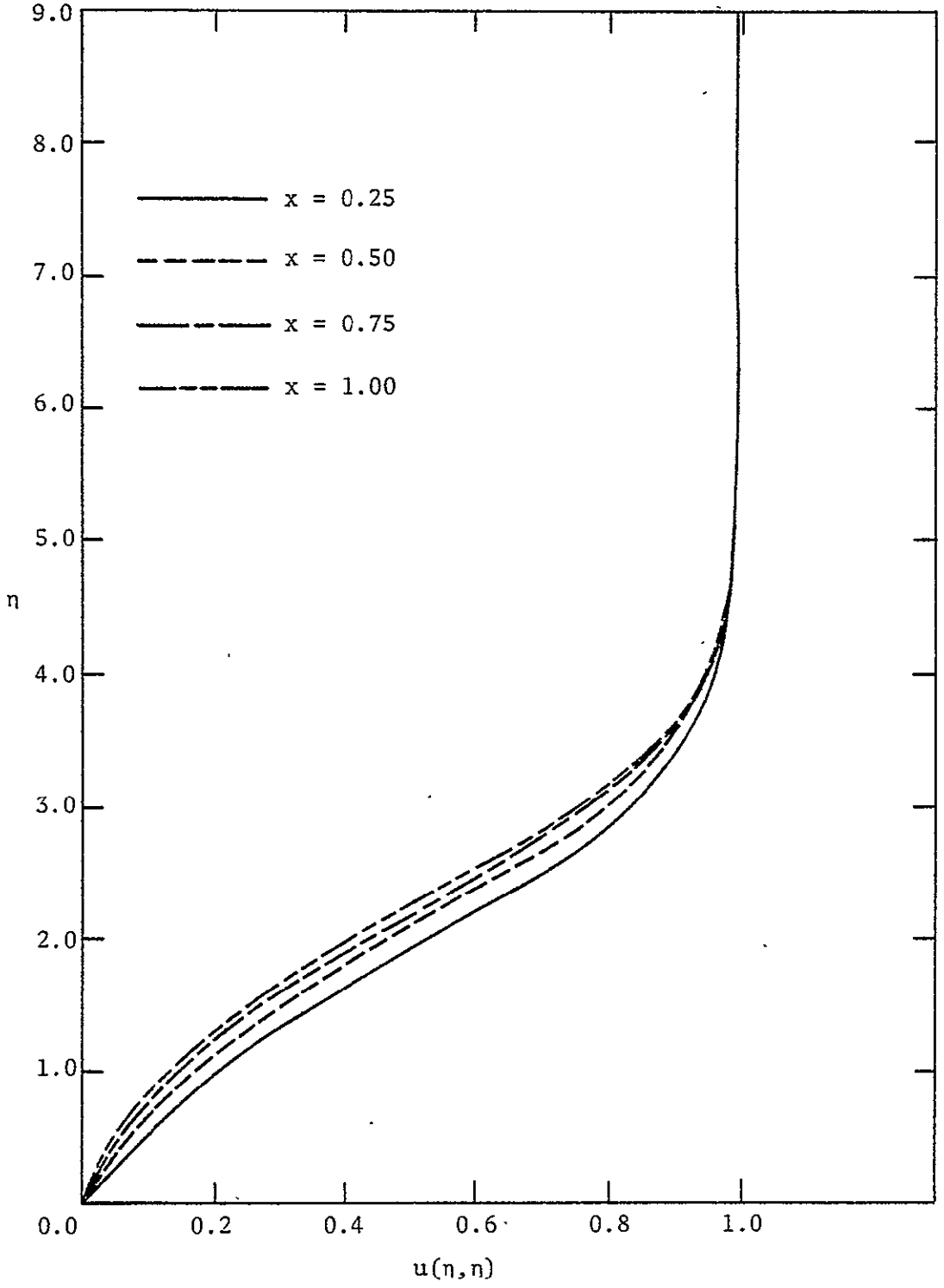

Figure 10. Effect of the axial distance on the axial velocity.

APPENDIX A

POTENTIAL FLOW SOLUTION

After Ghia and Davis (ref. 5) the three velocity components in dimensionless form are given by:

$$\tilde{u} = 1 - \frac{\beta}{2\sqrt{Re}} \left[\frac{y\left\{x^2 - y^2\right\}^{-1/2}}{\left\{ x + \sqrt{x^2 + y^2} \right\}^{1/2}} \right] - \frac{\beta}{2\sqrt{Re}} \left[\frac{z\left\{x^2 + z^2\right\}^{-1/2}}{\left\{ x + \sqrt{x^2 + z^2} \right\}^{1/2}} \right] \tag{A-1}$$

$$\tilde{v} = \tilde{v}(x,y) = \frac{\beta}{2\sqrt{Re}} \left[\frac{x + \sqrt{x^2 + y^2}}{x^2 + y^2} \right]^{1/2} \tag{A-2}$$

$$\tilde{w} = \tilde{w}(x,z) = \frac{\beta}{2\sqrt{Re}} \left[\frac{x + \sqrt{x^2 + z^2}}{x^2 + z^2} \right]^{1/2} \tag{A-3}$$

From (x,y,z) coordinate system $\tilde{u}$, $\tilde{v}$, and $\tilde{w}$ are transformed to the new coordinate (x,η,ζ) system, and the transformed velocity components, u, v, and w, respectively are obtained as:

$$u = 1 - \frac{\beta}{Re\ \sqrt{2}} \left[\frac{\eta \left\{ x + \frac{2\eta^2}{Re} \right\}^{-1/2}}{\left\{ x + \sqrt{x^2 + \frac{2\eta^2 x}{Re}} \right\}^{1/2}} \right]$$

$$- \frac{\beta}{Re\ \sqrt{2}} \left[\frac{\zeta \left\{ x + \frac{2\zeta^2}{Re} \right\}^{-1/2}}{\left\{ x + \sqrt{x^2 + \frac{2\zeta^2 x}{Re}} \right\}^{1/2}} \right] \qquad \text{(A-4)}$$

$$v = v(x,\eta) = \frac{\beta}{\sqrt{2}} \left[\frac{x + \sqrt{x^2 + \frac{2\eta^2 x}{Re}}}{x + \frac{2\eta^2}{Re}} \right]^{1/2} \qquad \text{(A-5)}$$

$$w = w(x,\zeta) = \frac{\beta}{\sqrt{2}} \left[\frac{x + \sqrt{x^2 + \frac{2\zeta^2 x}{Re}}}{x + \frac{2\zeta^2}{Re}} \right]^{1/2} \qquad \text{(A-6)}$$

The results obtained above are the same as those determined by Rubin (ref. 2) by using Green's function.

APPENDIX B

HALF AXIAL STEP - IMPLICIT IN η DIRECTION

$$2xu\frac{\partial u^*}{\partial x} - (u\eta - v)\frac{\partial u^*}{\partial \eta} - (u\zeta - w)\frac{\partial u^i}{\partial \zeta} = \frac{\partial^2 u^*}{\partial \eta^2} + \frac{\partial^2 u^i}{\partial \zeta^2} \tag{B-1}$$

$$2xu\frac{\partial v^*}{\partial x} - (u\eta - v)\frac{\partial v^*}{\partial \eta} - (u\zeta - w)\frac{\partial v^i}{\partial \zeta} - uv^* = -2x\frac{\partial p^*}{\partial \eta} + \frac{\partial^2 v^*}{\partial \eta^2} + \frac{\partial^2 v^i}{\partial \zeta^2} \tag{B-2}$$

$$2xu\frac{\partial w^*}{\partial x} - (u\eta - v)\frac{\partial w^*}{\partial \eta} - (u\zeta - w)\frac{\partial w^i}{\partial \zeta} - uw^* = -2x\frac{\partial p^i}{\partial \zeta} + \frac{\partial^2 w^*}{\partial \eta^2} + \frac{\partial^2 w^i}{\partial \zeta^2} \tag{B-3}$$

$$\frac{\partial^2 p^*}{\partial \eta^2} + \frac{\partial^2 p^i}{\partial \zeta^2} = \frac{1}{x}\left\{\left(2x\frac{\partial u^*}{\partial x} - \eta\frac{\partial u^*}{\partial \eta} - \zeta\frac{\partial u^i}{\partial \zeta}\right)\left(\frac{\partial v}{\partial \eta} + \frac{\partial w}{\partial \zeta}\right)\right.$$

$$+ \frac{\partial v}{\partial \eta}\frac{\partial w}{\partial \zeta} - \frac{\partial u}{\partial \eta}\left(2x\frac{\partial v^*}{\partial x} - \eta\frac{\partial v^*}{\partial \eta} - \zeta\frac{\partial v^i}{\partial \zeta} - v^*\right) \tag{B-4}$$

$$\left. - \frac{\partial v}{\partial \zeta}\frac{\partial w}{\partial \eta} - \frac{\partial u}{\partial \zeta}\left(2x\frac{\partial w^*}{\partial x} - \eta\frac{\partial w^*}{\partial \eta} - \zeta\frac{\partial w^i}{\partial \zeta} - w^*\right)\right\}$$

where the terms shown without superscripts are considered at the station (i+1/2). The variables shown by superscript * are considered unknown at station (i+1/2).

APPENDIX C

FULL AXIAL STEP - IMPLICIT IN ζ DIRECTION

$$2x\,u\,\frac{\partial u^{i+1}}{\partial x} - (u\eta - v)\,\frac{\partial u^{*}}{\partial \eta} - (u\zeta - w)\,\frac{\partial u^{i+1}}{\partial \zeta} = \frac{\partial^2 u^{*}}{\partial \eta^2} + \frac{\partial^2 u^{i+1}}{\partial \zeta^2} \qquad \text{(C-1)}$$

$$2x\,u\,\frac{\partial v^{i+1}}{\partial x} - (u\eta - v)\,\frac{\partial v^{*}}{\partial \eta} - (u\zeta - w)\,\frac{\partial v^{i+1}}{\partial \zeta} - uv^{*}$$

$$= -2x\,\frac{\partial p^{*}}{\partial \eta} + \frac{\partial^2 v^{*}}{\partial \eta^2} + \frac{\partial^2 v^{i+1}}{\partial \zeta^2} \qquad \text{(C-2)}$$

$$2x\,u\,\frac{\partial w^{i+1}}{\partial x} - (u\eta - w)\,\frac{\partial w^{*}}{\partial \eta} - (u\zeta - w)\,\frac{\partial w^{i+1}}{\partial \zeta} - uw^{*}$$

$$= -2x\,\frac{\partial p^{i+1}}{\partial \zeta} + \frac{\partial^2 w^{*}}{\partial \eta^2} + \frac{\partial^2 w^{i+1}}{\partial \zeta^2} \qquad \text{(C-3)}$$

$$\frac{\partial^2 p^{*}}{\partial \eta^2} + \frac{\partial^2 p^{i+1}}{\partial \zeta^2} = \frac{1}{x}\left\{\left(2x\,\frac{\partial u^{i+1}}{\partial x} - \eta\,\frac{\partial u^{*}}{\partial \eta} - \zeta\,\frac{\partial u^{i+1}}{\partial \zeta}\right)\left(\frac{\partial v}{\partial \eta} + \frac{\partial w}{\partial \zeta}\right)\right.$$

$$+ \frac{\partial v}{\partial \eta}\,\frac{\partial w}{\partial \zeta} - \frac{\partial u}{\partial \eta}\left(2x\,\frac{\partial v^{i+1}}{\partial x} - \eta\,\frac{\partial v^{*}}{\partial \eta} - \zeta\,\frac{\partial v^{i+1}}{\partial \zeta} - v^{*}\right) \qquad \text{(C-4)}$$

$$\left. - \frac{\partial v}{\partial \zeta}\,\frac{\partial w}{\partial \eta} - \frac{\partial u}{\partial \zeta}\left(2x\,\frac{\partial w^{i+1}}{\partial x} - \eta\,\frac{\partial w^{*}}{\partial \eta} - \zeta\,\frac{\partial w^{i+1}}{\partial \zeta} - w^{*}\right)\right\}$$

where the terms shown without superscripts are considered at the station (i+1/2). The variables shown by the superscript * are considered known at station (i+1/2). The variables shown by the superscript (i+1) are only the unknown variables at station (i+1).

APPENDIX D

MATRIX COEFFICIENTS OF THE LINEARIZED DIFFERENCE EQUATIONS

METHOD (a)

For the first half of the ADI procedure, from a location i to the intermediate * location, the components of matrices (A), (B), (C), and the vector $\vec{D}$ of the set of equations of Appendix B are as follows:

$$a_{11} = \frac{(u\eta - v)\lambda^2}{(\lambda + 1)\Delta\eta_+} - \frac{2\lambda}{(\lambda + 1)\Delta\eta_+^2} \tag{D-1}$$

$$a_{12} = 0 \tag{D-2}$$

$$a_{13} = 0 \tag{D-3}$$

$$a_{14} = 0 \tag{D-4}$$

$$a_{21} = 0 \tag{D-5}$$

$$a_{22} = a_{11} \tag{D-6}$$

$$a_{23} = 0 \tag{D-7}$$

$$a_{24} = -\frac{2\lambda^2 x}{(\lambda + 1)\Delta\eta_+} \tag{D-8}$$

$$a_{31} = 0 \tag{D-9}$$

$$a_{32} = 0 \tag{D-10}$$

$$a_{33} = a_{11} \tag{D-11}$$

$$a_{34} = 0 \tag{D-12}$$

$$a_{41} = \frac{1}{x}\left\{\frac{\partial v}{\partial \eta} + \frac{\partial w}{\partial \zeta}\right\} \frac{\eta\lambda^2}{(\lambda + 1)\Delta\eta_+} \tag{D-13}$$

$$a_{42} = -\frac{1}{x}\frac{\partial u}{\partial \eta}\left\{\frac{\eta\lambda^2}{(\lambda + 1)\Delta\eta_+}\right\} \tag{D-14}$$

$$a_{43} = -\frac{1}{x}\frac{\partial u}{\partial \zeta}\left\{\frac{\eta\lambda^2}{(\lambda + 1)\Delta\eta_+}\right\} \tag{D-15}$$

$$a_{44} = -\frac{2\lambda}{(\lambda + 1)\Delta\eta_+^2} \tag{D-16}$$

$$b_{11} = \frac{4xu}{\Delta x} - \frac{(u\eta - v)(\lambda - 1)}{\Delta\eta_+} + \frac{2}{\Delta\eta_+^2} \tag{D-17}$$

$$b_{12} = 0 \tag{D-18}$$

$$b_{13} = 0 \tag{D-19}$$

$$b_{14} = 0 \tag{D-20}$$

$$b_{21} = 0 \tag{D-21}$$

$$b_{22} = b_{11} - u^{i+1/2} \tag{D-22}$$

$$b_{23} = 0 \tag{D-23}$$

$$b_{24} = \frac{2x(\lambda - 1)}{\Delta\eta_+} \tag{D-24}$$

$$b_{31} = 0 \tag{D-25}$$

$$b_{32} = 0 \tag{D-26}$$

$$b_{33} = b_{22} \tag{D-27}$$

$$b_{34} = 0 \tag{D-28}$$

$$b_{41} = \frac{1}{x}\left\{\frac{\partial v}{\partial \eta} + \frac{\partial w}{\partial \zeta}\right\}\left\{\frac{4x}{\Delta x} - \frac{\eta(\lambda - 1)}{\Delta \eta_+}\right\} \tag{D-29}$$

$$b_{42} = \frac{1}{x}\frac{\partial u}{\partial \eta}\left\{\frac{4x}{\Delta x} - \frac{\eta(\lambda - 1)}{\Delta \eta_+} - 1\right\} \tag{D-30}$$

$$b_{43} = \frac{1}{x}\frac{\partial u}{\partial \zeta}\left\{\frac{4x}{\Delta x} - \frac{\eta(\lambda - 1)}{\Delta \eta_+} - 1\right\} \tag{D-31}$$

$$b_{44} = \frac{2}{\Delta \eta_+^2} \tag{D-32}$$

$$c_{11} = -\frac{(u\eta - v)}{(\lambda + 1)\Delta \eta_+} - \frac{2}{(\lambda + 1)\Delta \eta_+^2} \tag{D-33}$$

$$c_{12} = 0 \tag{D-34}$$

$$c_{13} = 0 \tag{D-35}$$

$$c_{14} = 0 \tag{D-36}$$

$$c_{21} = 0 \tag{D-37}$$

$$c_{22} = c_{11} \tag{D-38}$$

$$c_{23} = 0 \tag{D-39}$$

$$c_{24} = \frac{2x}{(\lambda + 1)\Delta n_+} \tag{D-40}$$

$$c_{31} = 0 \tag{D-41}$$

$$c_{32} = 0 \tag{D-42}$$

$$c_{33} = c_{11} \tag{D-43}$$

$$c_{34} = 0 \tag{D-44}$$

$$c_{41} = \frac{1}{x}\left\{\frac{\partial v}{\partial \eta} + \frac{\partial w}{\partial \zeta}\right\} \frac{\eta}{(\lambda + 1)\Delta\eta_+} \tag{D-45}$$

$$c_{42} = -\frac{1}{x} \frac{\partial u}{\partial \eta} \frac{\eta}{(\lambda + 1)\Delta\eta_+} \tag{D-46}$$

$$c_{43} = -\frac{1}{x} \frac{\partial u}{\partial \zeta} \frac{\eta}{(\lambda + 1)\Delta\eta_+} \tag{D-47}$$

$$c_{44} = -\frac{2}{(\lambda + 1)\Delta\eta_+^2} \tag{D-48}$$

$$d_1 = \frac{4xuu^i}{\Delta x} + (u\zeta - w) \frac{\partial u^i}{\partial \zeta} + \frac{\partial^2 u^i}{\partial \zeta^2} \tag{D-49}$$

$$d_2 = \frac{4xuv^i}{\Delta x} + (u\zeta - w) \frac{\partial v^i}{\partial \zeta} + \frac{\partial^2 v^i}{\partial \zeta^2} \tag{D-50}$$

$$d_3 = \frac{4xuw^i}{\Delta x} + (u\zeta - w) \frac{\partial w^i}{\partial \zeta} + \frac{\partial^2 w^i}{\partial \zeta^2} - 2x \frac{\partial p^i}{\partial \zeta} \tag{D-51}$$

$$d_4 = \frac{\partial^2 p^i}{\partial \zeta^2} + \frac{\zeta}{x} \frac{\partial u^i}{\partial \zeta} \left\{\frac{\partial v}{\partial \eta} + \frac{\partial w}{\partial \zeta}\right\} - \frac{\partial v}{\partial \eta} \frac{\partial w}{\partial \zeta} + \frac{\partial v}{\partial \zeta} \frac{\partial w}{\partial \eta}$$

$$+ \frac{\zeta}{x} \frac{\partial u}{\partial \eta} \frac{\partial v^i}{\partial \zeta} + \frac{\zeta}{x} \frac{\partial u}{\partial \zeta} \frac{\partial w^i}{\partial \zeta} \tag{D-52}$$

where the unsubscripted field variables are evaluated at the point (i+1/2,j,k) by the extrapolation equation (34) during first iteration and by the interpolation after one iteration using the calculated new value of previous iteration.

For the second half of the ADI procedure, from the location * to the (i+1) location, the same standard procedure is adopted. Here the derivatives of η are denoted by *, and they are assumed known, and the derivatives of ζ are assumed at station (i+1)′ and are assumed unknown. Thus, for the second half of the ADI procedure the elements of the matrices (A), (B), (C), and the vector $\vec{D}$ are not given.

APPENDIX E

MATRIX COEFFICIENTS OF THE LINEARIZED DIFFERENCE EQUATIONS

METHOD (b)

As discussed in the Numerical Analysis Section, in this approach the equations (18) to (20) are solved by the ADI method assuming the known pressure values. Thus, the three equations make the block matrices of size 3 × 3. The elements of the block matrices (A), (B), and (C) are identical to those of Appendix D. The constant vector $\vec{D}$ is slightly different, and the elements of vector $\vec{D}$ are given below.

$$d_1 = \frac{4xuu^i}{\Delta x} + (u\zeta - w)\frac{\partial u^i}{\partial \zeta} + \frac{\partial^2 u^i}{\partial \zeta^2} \qquad \text{(E-1)}$$

$$d_2 = \frac{4xuv^i}{\Delta x} + (u\zeta - w)\frac{\partial v^i}{\partial \zeta} + \frac{\partial^2 v^i}{\partial \zeta^2} - 2x\frac{\partial p}{\partial \eta} \qquad \text{(E-2)}$$

$$d_3 = \frac{4xuv^i}{\Delta x} + (u\zeta - w)\frac{\partial w^i}{\partial \zeta} + \frac{\partial^2 w^i}{\partial \zeta^2} - 2x\frac{\partial p}{\partial \zeta} \qquad \text{(E-3)}$$

A similar approach is adopted during the second half of the ADI procedure. During both, the procedures $\frac{\partial p}{\partial \eta}$ and $\frac{\partial p}{\partial \zeta}$ are computed at (i+1/2,j,k).

The pressure is calculated from equation (21) after obtaining the solution of u, v, and w from equations (18) to (20) by the explicit method. The Gauss-Siedel method is used for solution of the pressure equation. The complete expression for pressure calculation is as follows:

$$p_{j,k}^{n+1} = \frac{\Delta\zeta^2\left(p_{j+1,k}^{n} + \lambda p_{j-1,k}^{n}\right) + \Delta\eta^2\left(p_{j,k+1}^{n} + \lambda p_{j,k-1}^{n}\right)}{(\lambda + 1)(\Delta\eta^2 + \Delta\zeta^2)}$$

$$- \frac{\Delta\eta^2\,\Delta\zeta^2}{2X(\Delta\eta^2 + \Delta\zeta^2)} \left\{ \left(2x \frac{\partial u}{\partial x} - \eta \frac{\partial u}{\partial \eta} - \zeta \frac{\partial u}{\partial \zeta}\right) \left(\frac{\partial v}{\partial \eta} + \frac{\partial w}{\partial \zeta}\right) \right.$$

$$+ \frac{\partial v}{\partial \eta}\frac{\partial w}{\partial \zeta} - \frac{\partial u}{\partial \eta} \left(2x \frac{\partial v}{\partial x} - \eta \frac{\partial v}{\partial \eta} - \zeta \frac{\partial v}{\partial \zeta} - v\right) \qquad \text{(E-4)}$$

$$\left. - \frac{\partial v}{\partial \zeta}\frac{\partial w}{\partial \eta} - \frac{\partial u}{\partial \zeta} \left(2x \frac{\partial w}{\partial x} - \eta \frac{\partial w}{\partial \eta} - \zeta \frac{\partial w}{\partial \zeta} - w\right) \right\}$$

REFERENCES

1. Carrier, G.: The Boundary Layer in a Corner. Quarterly of Applied Mathematics, Vol. 4, No. 4 (1947), pp. 367-378.

2. Rubin, S.G.: Incompressible Flow Along a Corner. J. Fluid Mech., Vol. 26, Part 1 (1966), pp. 97-110.

3. Pal, A. and Rubin, S.G.: Asymptotic Features of the Viscous Flow Along a Corner. Quarterly of Applied Mathematics, Vol. 29 (April 1971), pp. 91-108.

4. Rubin, S.G. and Grossman, B: Viscous Flow Along a Corner: Numerical Solution of the Corner Layer Equations. Quarterly of Applied Mathematics, Vol. 29, No. 2 (July 1971), pp. 169-186.

5. Ghia, K.N. and Davis, R.T.: Numerical Solution of Corner Flow Problem Using an Alternating Direction Implicit Method. ARL 73-0119, U.S. Air Force (July 1973).

6. Nardo, C.T. and Cresci, R.J.: An Alternating Directional Implicit Scheme for Three-Dimensional Hypersonic Flows. J. Comput. Phys., Vol. 8, No. 2 (October 1971), pp. 268-284.

7. Peaceman, D.W. and Rachford, H.H., Jr.: The Numerical Solution of Parabolic and Elliptic Differential Equations. J. Soc. Ind. & Appl. Math., Vol. 3, No. 1 (March 1955), pp. 28-41.

8. Rubin, S.G. and Lin, T.C.: Numerical Methods for Two- and Three-Dimensional Viscous Flow Problems: Application of Hypersonic Leading Edge Equations. AFOSR-TR-71-0778, U.S. Air Force (April 1971). (Available from DDC as AD 726 547.)

9. Patankar, S.W. and Spalding, D.B.: A Calculation Procedure for Heat, Mass and Momentum Transfer in Three-Dimensional Parabolic Flows. Int. J. Heat and Mass Transfer, Vol. 15, No. 10 (October 1972), pp. 1787-1806.

10. Lewellen, W.S.; Teske, M.; and Donaldson, Coleman duP.: Turbulent Wakes in a Stratified Fluid, Part I: Model Development, Verification and Sensitivity to Initial Conditions. Rep. No. 226, Aeronaut. Res. Assoc., Princeton, Inc. (August 1972).

11. Van Dyke, M.: Perturbation Method in Fluid Mechanics. Academic Press, 1964.

12. Roach, P.J.: Computational Fluid Dynamics. Hermosa Publishers, 1972.

13. McDonald, H. and Briley, W.R.: Three-Dimensional Supersonic Flow of a Viscous or Inviscid Gas. J. Comput. Phys., Vol. 19 (1975), pp. 150-178.